

Identification and Feed-forward Control of Piezoelectric Bender Using Hammerstein Hysteresis Model

Lenka Kuklišová Pavelková^[0000–0001–5290–2389]
Květoslav Belda^[0000–0002–1299–7704]

Department of Adaptive Systems
The Czech Academy of Sciences, Institute of Information Theory and Automation
Pod Vodárenskou věží 4, 182 00, Prague 8, Czech Republic
pavelkov@utia.cas.cz, belda@utia.cas.cz

Abstract. The paper presents a modelling and identification of a piezoelectric actuator and the feed-forward controller design. A commercial piezoelectric bender, model PL140, from Physik Instrumente Co. is considered. Its physical model is derived using Euler-Bernoulli beam theory. The model is designed to generate experimental data without using a real actuator. Nevertheless, this model is unsuitable for control design due to its complex structure. For the purpose of control, a Hammerstein model is proposed. Its structure comprises a static non-linear component that characterizes hysteresis and a dynamic linear component represented by a stochastic auto-regressive model with external inputs (ARX model). The non-linear component of the Hammerstein model is represented by a shallow neural network. The parameters of the ARX model are estimated by the Bayesian approach. The feedforward controller is based on the independently inverted part of the developed Hammerstein model. The results are illustrated by simulations using the proposed physical model.

Keywords: Piezoceramic actuator · Hammerstein model · Hysteresis · ARX model · Bounded noise · Bayesian estimation · Feed-forward controller · Physical modelling · Euler–Bernoulli beam theory.

1 Introduction

Current developments in materials science are driven by the demand for innovative applications and devices. Piezoelectric actuator (PEA) is such a type of device. It has significant potential as an active structural component of micromanipulators across different fields of electronics and biomedicine [6].

Principle of PEA consists in electro-mechanical coupling, inverse piezoelectric effect, through which input electrical energy is converted into output force or motion. Piezoelectric materials are in the form of single crystals, piezoelectric ceramics (PZT) or polymers. For a precise positioning, PZT is mostly used due to a favourable ratio of input energy and range of motion [20].

The precision of the motion is significantly influenced by the inherent non-linearity of PEAs under dynamic operating conditions. This non-linearity is mainly due to hysteresis. Therefore, appropriate modelling methods able to handle this type of nonlinearity are required [10]. The behaviour of materials can be represented utilizing continuum mechanics. However, the associated partial differential equations are too complex for direct analytical solution. Consequently, numerical computations utilizing the finite element method (FEM) are employed to resolve these equations in a computationally efficient manner [8].

While the developed model is suitable for simulation, it remains too complex for control tasks. Consequently, alternative, simpler approximate models are being investigated for the non-linear modelling of PZT actuators. They integrate black-box modelling with a physical understanding of systems exhibiting hysteresis [9]. They can be represented through operator superposition or differential equations [5]. In this context, a Bouc-Wen (BW) model, belonging to the second group, is often used [9]. As it only describes a static relationship, it is frequently augmented with a dynamic linear component, such as transfer function or an auto-regressive model with external inputs (ARX model). This combination of static non-linear and dynamic linear components corresponds to the Hammerstein model concept [5]. Currently, the required control model is also often identified using artificial neural networks (ANNs) [17].

This paper builds on results presented in [12]. There, two mathematical models of the commercial piezoelectric bender PL140 of Physik Instrumente (PI) Co. were developed: (i) a physically based Simulink model, a substitute of the real piezo bender, aimed to serve as a data generator without the need for a real piezoelectric actuator, and (ii) a data-driven Hammerstein model to be used in control problems. The aforementioned Hammerstein model is used to design a feedforward controller that compensates a hysteresis nonlinearity.

The paper is organized as follows. Section 2 deals with physical modelling and related simulation model of specific piezoelectric bender. In Section 3, an identification of a data-driven Hammerstein model is presented. Section 4 introduces a feed-forward controller. The simulation experiments using both physical and data-driven models are described in Section 5.

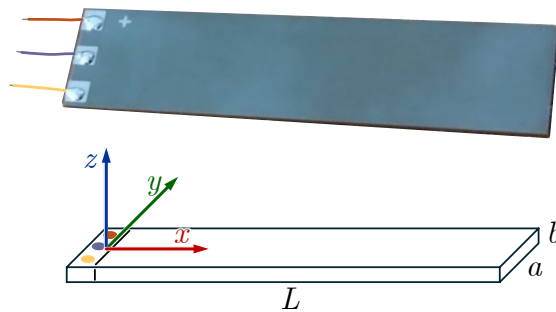


Fig. 1. PEA bender PL140 (top) and its main dimensions (bottom) [12]

2 PHYSICAL MODEL

This section summarises mathematical-physical modelling of the PEA. PICMA bender PL140 is considered as the PEA representative here, see Fig. 1. The result of the modelling is a model that is realised in MATLAB/Simulink. It serves as a substitute of the real PEA. In subsequent sections, static and dynamic analysis are introduced and the simulation model is described.

2.1 Static Model of Piezo Bender

Let the beam forming the piezo bender be as follows: (i) straight originally, and slight any taper; (ii) working only in linear elastic deformation; (iii) slender that length ℓ ($= L/n$, number of segments $n = 1$ here) to height (thickness) b ratio greater than 10; (iv) with only small deflections, less than 1/10 of the span, and additionally: (v) regular and homogeneous, and (vi) stressed by a uniform load. Then, in this case, the equation governing the beam's deflection z (designation according to deflections in z -axis) can be approximated simply using full differential equation of deflection line:

$$z^{IV}(\xi) = -\frac{q}{E J_y} \quad (1)$$

where E is the Young's modulus and J_y is quadratic moment of cross-section for neutral axis y , $J_y = bh^3/12$. Thereafter, it can be written the following:

$$q(\xi) = E J_y z^{IV}(\xi) = -q = \text{const.} \quad (2)$$

where q is a uniform load (force per unit length). Then, by the integration relative to position ξ , the following is obtained:

$$\begin{aligned} T(\xi) &= E J_y z^{III}(\xi) = -\int q(\xi) d\xi = -\int q d\xi = q\xi + c_1; \quad T(0) = 0 \Rightarrow c_1 = 0 \\ T(\xi) &= q\xi; \quad x = l - \xi, \quad dx = -d\xi, \quad \xi = l - x \Rightarrow T(x) = q(l - x) \end{aligned} \quad (3)$$

where $T(x)$ is a shear force. In similar way, it is possible to obtain:

$$\begin{aligned} M(\xi) &= E J_y z^{II}(\xi) = -\int T(\xi) d\xi = -\int q\xi d\xi = \frac{q}{2}\xi^2 + c_2; \quad M(0) = 0 \Rightarrow c_2 = 0 \\ M(\xi) &= -\frac{1}{2}q\xi^2, \quad \xi = l - x \Rightarrow M(x) = -\frac{1}{2}q(l - x)^2 \end{aligned} \quad (4)$$

where $M(x)$ is a bending moment. Furthermore, subsequent integration is:

$$\begin{aligned} \varphi(\xi) &= z^I(\xi) = -\int \frac{M(\xi)}{E J_y} d\xi = -\frac{1}{E J_y} \int -\frac{1}{2}q\xi^2 d\xi = \frac{1}{E J_y} \frac{q}{6} \xi^3 + c_3 \\ \varphi(\ell) &= 0 \Rightarrow c_3 = -\frac{1}{E J_y} \frac{q}{6} \ell^3, \quad \varphi(\xi) = -\frac{1}{E J_y} \frac{q}{6} (\xi^3 - \ell^3), \quad \xi = l - x \Rightarrow \\ \varphi(x) &= -\frac{1}{E J_y} \frac{q}{6} ((l - x)^3 - \ell^3) \end{aligned} \quad (5)$$

where $\varphi(x)$ is a bending angle.

Finally, the last integration leads to:

$$\begin{aligned}
 z(\xi) &= -\int \varphi(\xi) d\xi = \frac{1}{E J_y} \frac{q}{6} \int (\xi^3 - \ell^3) d\xi = -\frac{1}{E J_y} q \left(\frac{1}{24} \xi^4 - \frac{1}{6} \ell^3 \xi \right) + c_4 \\
 z(\ell) = 0 &\Rightarrow c_4 = \frac{1}{E J_y} q \left(\frac{\ell^4}{24} - \frac{\ell^4}{6} \right) = -\frac{1}{E J_y} \frac{3}{24} q \ell^4 = -\frac{1}{8} \frac{q \ell^4}{E J_y} \\
 z(\xi) &= -\frac{1}{E J_y} q \left(\frac{1}{24} \xi^4 - \frac{1}{6} \ell^3 \xi + \frac{1}{8} \ell^4 \right), \quad \xi = l - x \Rightarrow \\
 z(x) &= -\frac{q}{E J_y} \left(\frac{1}{24} (\ell - x)^4 - \frac{1}{6} \ell^3 (\ell - x) + \frac{1}{8} \ell^4 \right) \tag{6}
 \end{aligned}$$

where $z(x)$ is a bending deflection. For static deflection modelling, the relation between a uniform load q and input voltage u is necessary to calibrate. An illustration of the obtained formulas (2)-(6) is depicted in Fig. 2, for values in Table 1.

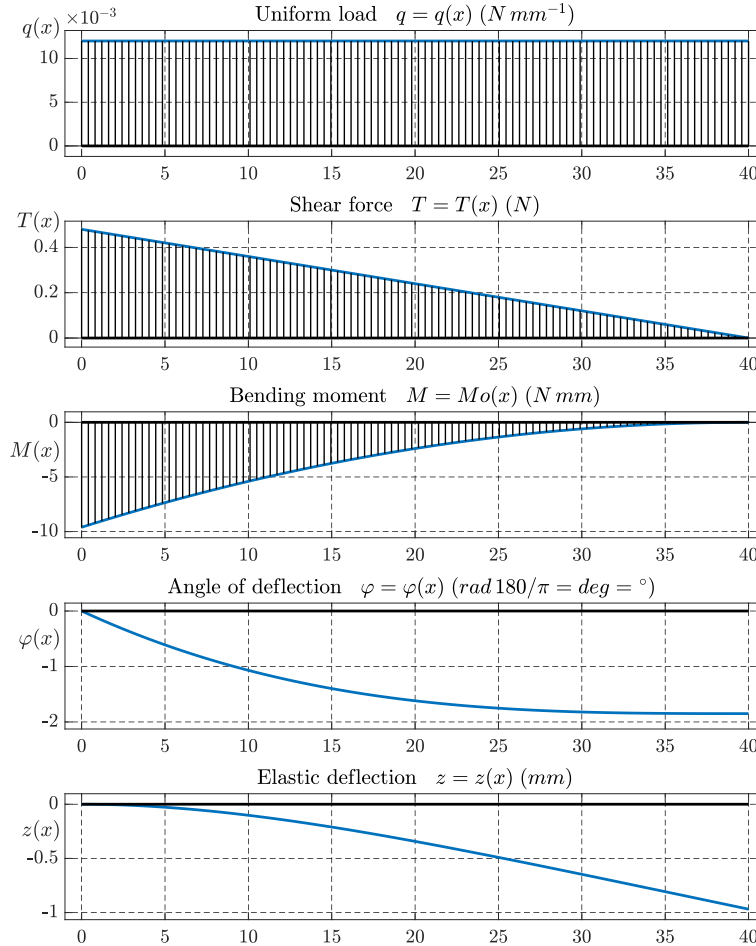


Fig. 2. Courses of static force effects and deflection quantities

2.2 Dynamic Model Beam Theory for Piezo Bender

Transient or dynamic behaviour of real physical deformable bodies can be described using the general theory of continuum mechanics [4]. Considering a prism-shaped piezo bender (Fig. 1), a beam, a simplification by Euler-Bernoulli beam theory can be used [15]. This theory will be considered and applied to model construction in this section. The obtained model is considered as a model substituting a real piezo ceramic beam. We consider that used PEA is built from a homogeneous isotropic linear elastic piezoceramic material. Its stress σ is related to the strain ε by $\sigma = E \varepsilon$, where E is already mentioned the Young's modulus. Then, general constitutive equations [4] considering strains in space are:

$$\sigma = C \varepsilon - e^T E_o \quad (7)$$

$$d = e \varepsilon + \epsilon E_o \quad (8)$$

where E_o , C , ε , e , d and ϵ are the electric field, compliance tensor, strain field, electric displacement field, piezo stress coefficient tensor and permittivity tensor at constant or zero strain, respectively.

The required beam equations can be separated from (7) and (8). Let us proceed from strain along axis x (simplifying a general three-dimensional problem to a one-dimensional one, $\circ \rightarrow (x \wedge z)$, i.e. corresponding directions):

$$\varepsilon \rightarrow \varepsilon_{xx}(x, z) = -z \frac{d\varphi_y}{dx}(x) \quad (9)$$

$$E_o \rightarrow E_z = \frac{u}{b} \quad (10)$$

$$\sigma \rightarrow \sigma_{xx}(x, z) = -c_{11} z \frac{d\varphi_y}{dx}(x) - e_{31} \frac{u}{b} \quad (11)$$

where $c_{11} = E$ and E_z is electric field perpendicular to plane xy and u is input voltage of surface electrodes of PEA. Then, the moment from the stress field is

$$M_y(x) = - \iint z \sigma_{xx}(x, z) dS \quad (12)$$

Calculating the double integral in (12), the bending moment is expressed as:

$$M_y(x) = EI \frac{d\varphi_y}{dx}(x) + a b e_{31} u \quad (13)$$

where $I = 1/12 a b^3$ is the second moment of area of the rectangular cross-section. Let us continue by developing the equation for electric displacement (8), again simplifying to the relevant one-dimensional subspace, as:

$$d_z(x, z) = e_{31} \varepsilon_{xx}(x, z) + \epsilon E_z \quad (14)$$

$$d_z(x, z) = -e_{31} z \frac{d\varphi_y}{dx}(x) + \epsilon \frac{u}{b} \quad (15)$$

$$dq = \iint d_z dS = e_{31} a b d\varphi_y \quad (16)$$

where dq is infinitesimal accumulated bend charge, given by a bend angle change. Thus, the charge q for a specific bend can be expressed as follows

$$q = e_{31} a b (\varphi_y(x_{k+1}) - \varphi_y(x_k)) \quad (17)$$

Then, the resulting Euler-Bernoulli beam equations for torque and charge are:

$$M_y(x) = E I \frac{d\varphi_y}{dx}(x) + a b e_{31} u \quad (18)$$

$$q = e_{31} a b (\varphi_y(x_{k+1}) - \varphi_y(x_k)) + \frac{\epsilon a \ell}{b} u \quad (19)$$

The equations (13)-(19) leads to the state-space finite-element form (22) of one element of the modelled beam divided into n elements:

$$\begin{bmatrix} F_C \\ \tau_C \\ F_R \\ \tau_R \end{bmatrix} = K \begin{bmatrix} z_C \\ \varphi_C \\ z_R \\ \varphi_R \end{bmatrix} \quad (20)$$

$$\left[\begin{array}{c|c} \bar{M} & 0 \\ \hline 0 & 0 \end{array} \right] \begin{bmatrix} \ddot{x} \\ 0 \end{bmatrix} + \left[\begin{array}{c|c} K & v_{\text{piezo}} \\ \hline -v_{\text{piezo}}^T & \delta_{\text{piezo}} \end{array} \right] \begin{bmatrix} x \\ u \end{bmatrix} = \begin{bmatrix} f \\ q \end{bmatrix} \quad (21)$$

where

$$K = \frac{E I}{\ell^3} \begin{bmatrix} 12 & 6\ell & -12 & 6\ell \\ 6\ell & 4\ell^2 & -6\ell^2 & 2\ell^2 \\ -12 & -6\ell & 12 & -6\ell \\ 6\ell & 2\ell^2 & -6\ell & 4\ell^2 \end{bmatrix}, \quad \bar{M} = \frac{m}{420} \begin{bmatrix} 156 & 22\ell & 54 & -13\ell \\ 22\ell & 4\ell^2 & 13\ell & -3\ell^2 \\ 54 & 13\ell & 156 & -22\ell \\ -13\ell & -12\ell & -22\ell & 4\ell^2 \end{bmatrix}$$

$$v_{\text{piezo}} = [0 \quad e_{31} a b \quad 0 \quad -e_{31} a b]^T, \quad \delta_{\text{piezo}} = \frac{\epsilon a \ell}{b}$$

with added dumping matrix B , the final form is

$$M \begin{bmatrix} \ddot{x} \\ 0 \end{bmatrix} + B \begin{bmatrix} \dot{x} \\ 0 \end{bmatrix} + \bar{K} \begin{bmatrix} x \\ u \end{bmatrix} = \begin{bmatrix} f \\ q \end{bmatrix} \quad (22)$$

where $m = \rho a b \ell$ is the element mass with density ρ and ℓ as element length and $L = n \ell$ total beam length, a and b are cross-sectional parameters: width and thickness respectively (see Fig. 1), $x = [z_C \varphi_C z_R \varphi_R]^T$ is generalized coordinate vector, e_{31} is a piezoelectric stress-charge coupling element and ϵ is electrical permittivity. The set (22) can be numerically solved in n -element chain, where terms K , M , B ($=$ zero matrix but $b_{11} \neq 0$), q and $f = [F_C \tau_C F_R \tau_R]^T$ are stiffness matrix, mass matrix, stiffness finite element matrix, damping matrix, accumulated charge trough PEA and generalized force effects, respectively, with appropriate dimensions [3].

Table 1. Parameters of PL140 - PIC251 used in Simulink model in Fig. 3.

<i>Symbol</i>	<i>Description</i>	<i>Value</i>
L	length	40 mm
a	width	11 mm
b	thickness	0.55 mm
C_{piezo}	capacitance	8.2 μF
u_{rated}	rated voltage range	$\pm 30\text{ V}$
z_{free}	free deflection at u_{rated}	$\pm 1\text{ mm}$
F_{block}	blocking force at u_{rated}	$\pm 0.5\text{ N}$
f_n	first natural frequency	160 Hz

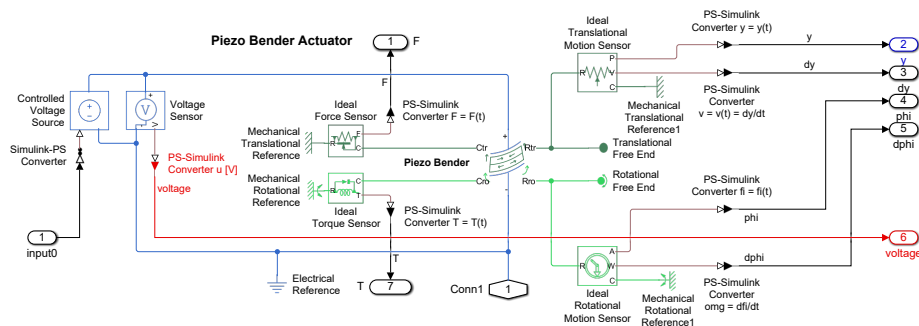
The relations between available datasheet and material parameters, in equations and in MATLAB/Simulink model, are summarised as follows [15]

$$e_{31} = -\frac{2\ell F_{\text{block}}}{3ab u_{\text{rated}}}, \quad E = -\frac{4F_{\text{block}}\ell^3}{z_{\text{free}}ab^3}, \quad \epsilon = \frac{b}{a\ell} \left(C_{\text{piezo}} + \frac{4F_{\text{block}}z_{\text{free}}}{u_{\text{rated}}^2} \right) \quad (23)$$

where parameters on the right sides of equations (23) are: F_{block} , a , b , u_{rated} , z_{free} and C_{piezo} – blocking force, dimensions, rated drive voltage and free deflection at u_{rated} , beam capacitance, respectively. Its values are summarised in Table 1.

2.3 Simscape Model

In the context of the mentioned physical analysis, MATLAB/Simulink with Simscape block libraries offers a convenient preconfigured way of building a simulation model of a real beam, as opposed to programming the equations above, see Fig. 3. This model consists of the main block of Piezo Bender block [13] that represents piezoelectric bimorph beam. It is connected through mechanical translational and rotational reference via ideal force and torque sensors to the ground on one side and on other side left free via translational and rotational free ends. They are connected with ideal translational and rotational motion sensors. Input voltage of PEA is provided by a controlled voltage source. The bending block simulates bending when an electric potential is applied across its layers and generates an electric potential when it is bent. This model (Fig. 3) is used in following sections. Note that the output signal is denoted y to be consistent with automatic control theory instead of the physical notation z in text above.


Fig. 3. Created Simulink model comprising Simscape blocks.

3 DATA DRIVEN MODEL

This section deals with an identification of a data-driven model of a PEA. For this purpose we have chosen a Hammerstein model [5]. It is suitable for modelling a PEA because its structure effectively separates the actuator's complex behaviour into two manageable parts. The model uses a static nonlinear function to describe the inherent hysteresis and connects it in series with a dynamic linear function that represents the frequency-dependent characteristics of the electromechanical system [19]. The mentioned linear function is frequently represented by a dynamic transfer function [5]. The Hammerstein model facilitates the analysis of a PEA by separating the nonlinear hysteresis component from the linear dynamic characteristics. It is also convenient to use in various control algorithms and simulation tools [7].

Fig. 4 shows a block diagram of the Hammerstein model. The block NLS specifies a static hysteresis nonlinearity, while the block LD represents a dynamic linear component of the piezoelectric actuator. The signals u_t , z_t , v_t , and y_t denote an input, an unobservable hidden variable, noise, and an output, respectively; $t \in \{1, 2, \dots, \bar{t}\}$ denotes a discrete time.

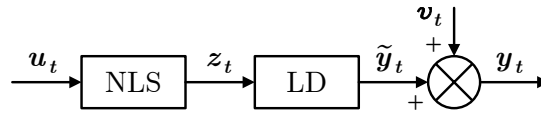


Fig. 4. Block diagram of Hammerstein model [12] consisting of a static nonlinear part NLS and a dynamic linear part LD that is influenced by an additive noise v_t

In general, there exists a dependency between the linear and the non-linear component of the Hammerstein model. This dependency has to be taken into account during identification. However, under specific conditions, the linear component can be isolated from the non-linear component and both parts can be identified independently [2]. The procedure starts with the identification of the LD part using a special signal that does not activate the nonlinearity. Then, LD part is used together with new output data y_t to estimate the hidden quantity z_t . Finally, using z_t and the relevant input data u_t , the NLS part is identified. This approach will be detailed in subsequent subsections.

3.1 Linear Dynamic part of Hammerstein model

The LD part of Hammerstein model (Fig. 4) is often represented by an autoregressive model with external input (ARX model) [5]. Here, we consider a stochastic ARX model of the second order, as it is a well established representation of electro-mechanical systems [18]. Further, the involved noise is assumed to be bounded and uniformly distributed. The advantage of this is that, contrary

to a model with normal noise, this model provides a guaranteed estimate, i.e. a set in which the estimated parameter is guaranteed to be located. Another benefit is that we do not need to know the statistical properties of the noise, but only its bounds.

The 2^{nd} order ARX model with a uniform noise is defined as follows

$$\begin{aligned} y_t &= a_1 y_{t-1} + a_2 y_{t-2} + b_0 u_t + b_1 u_{t-1} + b_2 u_{t-2} + v_t = \psi_t^T \theta + v_t \\ v_t &\sim \mathcal{U}_v(-r, r) \end{aligned} \quad (24)$$

where T denotes the transposition, y_t is an observable output, u_t is a known input, $\psi_t = [y_{t-1}, y_{t-2}, u_t, u_{t-1}, u_{t-2}]^T$ is a regression vector, $\theta = [a_1, a_2, b_0, b_1, b_2]^T$ is a vector of unknown regression coefficients, v_t is a uniform white noise, independent and identically distributed and $\mathcal{U}_v(-r, r)$ denotes a uniform distribution of v on the support $(-r, r)$.

Equivalently, the nominal part of ARX model (24), $\psi_t^T \theta$, can be described by the following transfer function

$$G_s(z^{-1}) = \frac{b_0 + b_1 z^{-1} + b_2 z^{-2}}{1 - a_1 z^{-1} - a_2 z^{-2}} \quad (25)$$

To estimate the regression coefficients of ARX model (24) from input-output data, we use the Bayesian approach [11]. There, a system of interest is described by the following probability density functions (pdfs):

$$\begin{aligned} \text{prior pdf } f(\Theta) &\equiv f(\Theta|d(0)), \\ \text{observation model } &f(y_t|u_t, d(t-1), \Theta), \end{aligned} \quad (26)$$

where Θ is an unknown parameters vector.

Bayesian parameter estimation consists in the recursive evolution of the posterior pdf $f(\Theta|d(t))$ that starts from the prior pdf $f(\Theta)$ (26):

$$f(\Theta|d(t)) \propto f(y_t|u_t, d(t-1), \Theta) f(\Theta|d(t-1)), \quad t \in \{1, 2, \dots, \bar{t}\} \quad (27)$$

where $d(t) = [d_t, d_{t-1}, \dots, d_1]$ is a sequence of observed data records, $d_t = (y_t, u_t)$, \propto means the equality up the normalising constant. Note that here is no formal distinction of a random variable, its realization and pdf argument.

By considering the ARX model (24) as the observation model (26), with Θ comprising both θ and r , the application of (27) results in gradually increasing complexity of the support of $f(\Theta|d(t))$. Therefore, an approximate solution has to be implemented.

In [14], the estimation algorithm is proposed that provides the approximate posterior pdf on parameters, $f(\Theta|d(t))$. Its support, represented by a polytope with a constant number of faces, recursively circumscribe the original complex support. The expected values of both the model regression parameters θ

and the noise bound r are obtained as follows:

$$\begin{aligned}\hat{\theta} &= \hat{r}v_{\psi}^{-1} [l_{n-1}, 0] \frac{u+l}{2} - v_{\psi}^{-1}v_y, \\ v &= \begin{bmatrix} v_{\psi} & v_y \\ 0 & 1 \end{bmatrix} \\ \hat{r} &= \frac{\alpha+1}{\alpha} \frac{1-\gamma^{\alpha}}{1-\gamma^{\alpha+1}} u_n^{-1}, \quad \gamma = \frac{\max(l_n, 0)}{u_n}.\end{aligned}\tag{28}$$

where α corresponds to the number of processed data, $[l_{n-1}, 0]$ denote $n-1$ rows of unit n matrix, column vectors l , u and the square matrix v are the approximate statistics that define the approximate support \hat{S}_t of $f(\Theta|d(t))$ as follows:

$$\hat{S}_t = \{\Theta : \Theta_n > 0, l \leq v\Theta \leq u\},\tag{29}$$

$\Theta_n = 1/r$ is the n -th entry of the vector $\Theta = [-\theta^T \Theta_n, \Theta_n]$. The matrix v has the upper triangular form with unit diagonal.

The update of \hat{S}_t consists of the extension of v by one row, which corresponds to the vector $\Psi_t = [\psi^T, y_t]$, and the extension of l by -1 and u by 1 . Then, the orthogonal rotation is performed, which zeroes the last rows of l , v , and u and maintains the triangular form of v . For algorithmic details see [14]. Note that the noise range r is estimated together with the model parameters, therefore it is not required to have a prior knowledge of it.

3.2 Nonlinear static part of Hammerstein model

The static nonlinear component of the Hammerstein model, NLS, can be identified using a dataset comprising u_t and z_t , as illustrated in Fig. 4. The inputs u_t are accessible. The hidden variables z_t can be predicted utilizing the inverse estimated ARX model that characterizes the LD component, together with the y_t produced by the Simscape model, Fig. 3, that is excited by the input signal u_t .

Since LD is described by the ARX model (24) with input z_t and output y_t , see Fig. 4, the inverse model with input y_t and output z_t is expressed as:

$$z_t = \frac{1}{b_0} (y_t - a_1 y_{t-1} - a_2 y_{t-2} - b_1 z_{t-1} - b_2 z_{t-2} - v_t) = \hat{z}_t - \frac{1}{b_0} v_t\tag{30}$$

where a_1 , a_2 , b_0 , b_1 and b_2 correspond to the regression parameters of the ARX model (24). Assuming the uniform noise v_t , z_t is uniformly distributed on the support $[\hat{z}_t - r/b_0, \hat{z}_t + r/b_0]$ with the mean \hat{z}_t .

The NLS part of Hammerstein model will be represented by a shallow neural network (NN) \mathcal{N} with input u_t , one hidden layer and output z_t , i.e.,

$$z_t = \mathcal{N}(u_t).\tag{31}$$

In MATLAB, \mathcal{N} is represented by a *idNeuralNetwork* object, which is defined by the number of hidden layers including number of nodes and activation function for each layer. Here, we have set structure of \mathcal{N} to consist of three layers with ‘‘tanh’’ activation function. For an identification of \mathcal{N} , the Matlab function *nlarx* is used.

3.3 Identification Procedure of Hammerstein model

This subsection will summarize the identification of the two parts of the Hammerstein model described above into a concise procedure.

The identification utilises two data sets, D_1 and D_2 , where inputs are described below and corresponding outputs are generated by Simscape model, depicted in Fig. 3:

- D1** – Input sequence in D_1 correspond to the pseudo-random binary sequence (PRBS). It is a signal that shifts between two levels in a certain pattern such that its mean value and covariance function are quite similar to those of a white noise process. It can be generated by using shift registers for realizing a finite state system, and is a periodic signal. The period is chosen to be of the same order as the number of samples in the experiment, or larger [16]. Using the PRBS input signal, the nonlinearity will not appear, as it remains unexcited [2]. As a consequence, the hidden variable z_t equals to u_t in Fig. 4, which allows to identify the linear component of LD independently of the nonlinear component.
- D2** – Data set D_2 is intended for the identification of the NLS part. Therefore, the input sequence in D_2 has to be sufficiently diversified. For this purpose, we have chosen sin wave input. Assuming that NLS is static and u_t and z_t are available (see Fig. 4), the structural information on the unknown NLS can be derived from its graphical representation [2]. We can estimate the hidden z_t using the output sequence in D_2 data set and inverted linear part LD that has been identified in the previous step by using the data set D_1 .

The complete identification of data-driven model of PL140 based on the Hammerstein model according to Fig. 4 is summarised as follows:

- i) generate data set D_1 using the Simscape model in Fig. 3, excited by the PRBS signal;
- ii) estimate the parameters of the LD block in the Hammerstein model, Fig. 4, using the data set D_1 and formula (28), whereas LD is represented by ARX model (24);

- iii) generate data set D_2 using the Simscape model, Fig. 3, excited by sin wave-form signal with amplitude corresponding to the maximum voltage value;
- iv) predict the z_t in Hammerstein model, Fig. 4, as outputs of the inverse ARX model (30) where the output sequence in D_2 plays the role of input data;
- v) identify the NLS block in Hammerstein model using input sequence in D_2 , output data \hat{z}_t from iv) and the mapping (31).

4 Feed-forward Controller

In this section, a feed-forward controller is proposed. It consists of a serial coupling of an inverse dynamic model and an inverse hysteresis model, see the block diagram in Fig. 5.

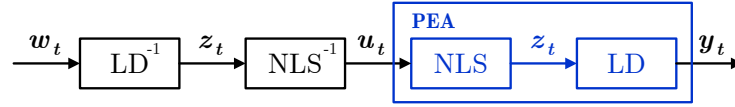


Fig. 5. Feedforward controller consisting of the inverse ARX model (LD^{-1}) and inverse hysteresis (NLS^{-1}) with reference w_t

4.1 Inverted LD part of Hammerstein model

The inverse ARX model LD^{-1} is already available. It is identical to the formula (30) used for the identification of NLS part in Hammerstein model, Fig. 4. In comparison to [12], we have added here a term b_0u_t to make the inverse model physically realizable in online mode. Note that model in [12] was only used for a one-time hysteresis identification where the whole data set was handled together, so the missing b_0 did not matter.

4.2 Inverted NLS part of Hammerstein model

The construction of the inverse hysteresis model NLS^{-1} is not so straightforward as relationship between involved variables z_t and u_t is non-linear. There are many numerical methods to invert non-linear functions. Here, we adopt a numerical technique based on optimal k-vector range searching [1]. This technique allows to invert one dimensional analytic or tabulated non-linear function, $z = g(x)$, in assigned ranges of interest. It needs to carry out initial preprocessing for each function but the inversion itself is then very fast. Therefore, the method is appropriate when multiple inversions of the same function are required, as is our case.

The offline preprocessing process involves the construction of a k-vector, i.e. the vector of indexes containing information about the nonlinearity of the sorted database. Specifically, the k-vector indicates the number of elements below a mapping function for specific values. The mapping function is a straight line that starts at the minimum and ends at the maximum.

Before k-vector is constructed, the non-linear function $z = g(x)$ has to be discretized and its output values sorted in the ascending order. Using the resulting sorting indexes, the inputs are rearranged according to the outputs. Also, the maximum absolute difference δ between consecutive y -values to define a searching range for root finding is computed.

Once the k-vector is built, the inversion of $z = g(x)$ can be performed online. To find a corresponding x value for a specific output z_r consists in finding roots $\{x_r\}$ of the equation

$$g(\{x_r\}) - z_r = 0. \quad (32)$$

For a given value z_r , the searching range $[z_a, z_b] = [z_r - \delta/2, z_r + \delta/2]$ is set. Then, the k-vector is used to find indices (k_a, k_b) corresponding to the searching range, which provide a subset of x -values (x_s) that are close to the roots.

The retrieved x -values are sorted and distinct roots are identified by checking the distance between consecutive x -values. If the distance is less than a threshold, they belong to the same root.

The above procedure cannot be used directly in our case. The resulting hysteresis curve is not a function, but can be divided into two parts corresponding to two nonlinear functions where the separator is the line passing through the turning points. Thus, we obtain two sets of inputs and outputs (databases), D_L and D_U , where D_L corresponds to the lower part of the curve and D_U corresponds to the upper part of the curve. We then create the corresponding k -vectors, k_L and k_U . For their subsequent use, we then need to add a decision rule for choosing the set to use. We assume the hysteresis property that the output response is delayed after the input signal. This means that if the current input value is higher than the previous one, then we use D_L and if it is lower, then we use D_U .

5 EXPERIMENTS

In this section, the results of Hammerstein model identification, Fig. 4, as presented in [12], are summarized, followed by the description of feed-forward controller setting and illustrating its performance.

5.1 Identification of Hammerstein model

Data for the identification of Hammerstein model are generated by the Simscape model of piezoelectric bender PL140, see Fig. 3. Through the input block 1 enter various input data that correspond to a voltage. Output deflection of piezoelectric bender is provided by the output block 2. The identification process is performed according to the procedure described in Subsection 3.3 with the sampling frequency $T_s = 10^{-3}$ s.

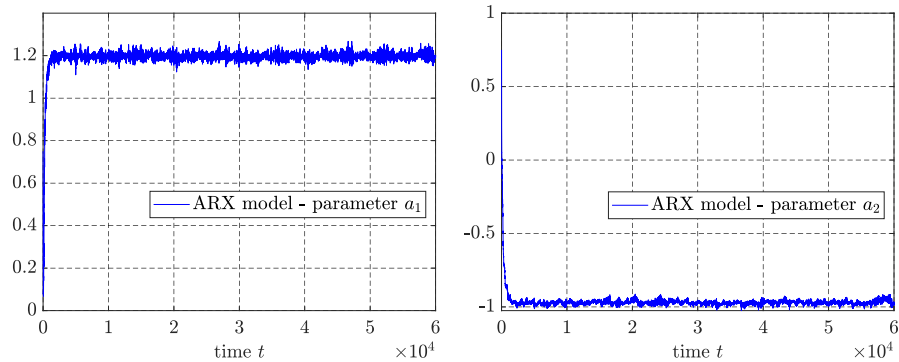


Fig. 6. The course of the parameter estimate a_1 (left) and a_2 (right) in ARX model (24)

Table 2. Point estimates of the ARX model (24) representing LD part in Fig. 4

a_1	a_2	b_0	b_1	b_2
1.196	-0.972	0.004	0.004	0.003

First, the D_1 data set, see Section 3.3, are generated for the subsequent estimation of the ARX model (24) parameters. As an example, the time courses of the regression coefficients a_1 and a_2 estimates are shown in Fig. 6. It is evident that while the estimates converge to specific values, they do not stabilize and instead oscillate around these values. The time courses of b_0 , b_1 and b_2 are similar.

The required point parameter estimates are set as the median values from the steady-state part of the relevant time courses. The specified values of all regression coefficients are summarised in the Table 2. Note that the paper [12] considers the 2nd order ARX model without zero delayed input. Here, we have added it to obtain physically feasible inverted ARX model, i.e. with output depending only on current and past inputs and outputs.

Second, the D_2 data set, see Section 3.3, are generated to be used for estimating the hidden variable z_t and the subsequent identification of the non-linear part NLS represented by (31). In the experiment, we have used a shallow neural network with three layers and the hyperbolic tangent activation function. Its structure is defined by the Matlab function *idNeuralNetwork*. Model parameters are then identified using MATLAB function *nlrx*.

The estimated hysteresis curve, i.e. relationship between the applied input voltage u and the mean of the hidden variable \hat{z} is depicted in the left part of Fig. 7.

5.2 Feed-forward Control

The proposed feed-forward controller (FFC), see Fig. 5, consists of LD^{-1} part (30) and NLS^{-1} part obtained by the procedure described in Section 4.2. The required splitting of hysteresis curve is depicted in the right part of Fig. 7.

The FFC was tested with a Simulink model, Fig. 3, as a substitute of the real piezo-bender PL140. We set the reference w_t as a sine wave with amplitude 1 that corresponds to the maximal catalogue deflection of PL140. Then, the output of feed-forward controller was computed, i.e., the input control sequence u_t , and fed into the Simulink model through input block 1. The part of simulation results are shown in Fig. 8 (left).

The performance of the controller is shown in Fig. 8 (right), where the static relationship between input voltage and output deflection is depicted and compared with the relationship between input to the NLS^{-1} block and output deflection.

The accuracy of the proposed compensator would be further improved by not using the roots (32) directly for the inversion, but instead to take them as an initial guess for another root finder, eg Newton-Raphson iterations.

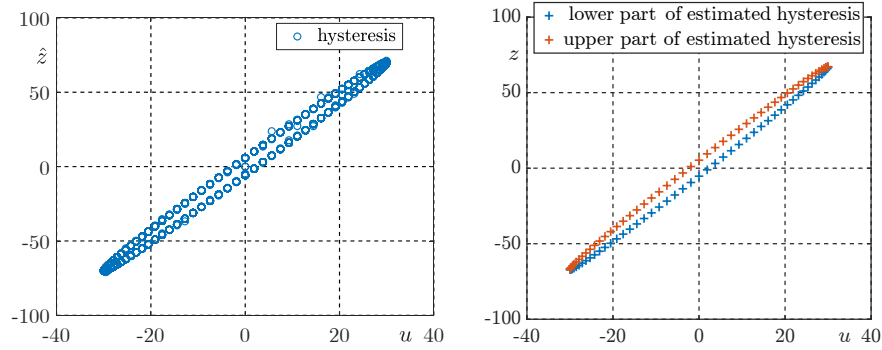


Fig. 7. Input-output representation of NLS part of Hammerstein model, Fig. 4 (hysteresis), [12] (left) and splitting of the hysteresis curve into two non-linear functions with averaged z -values (right)

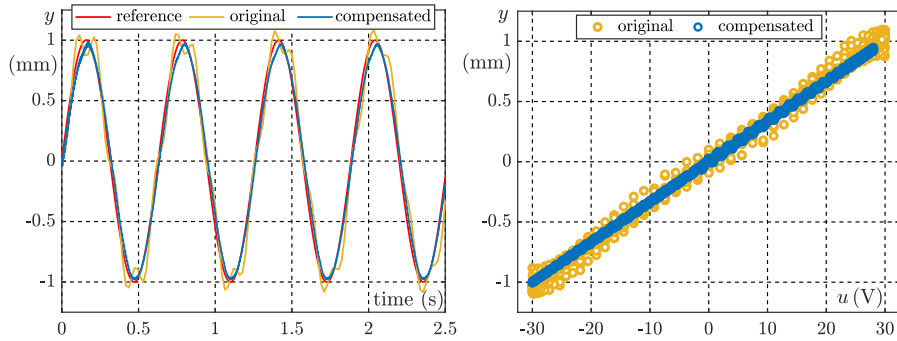


Fig. 8. Part of the time course of the feed-forward control of PEA – blue (left) and relationship between input voltage and piezo actuator deflection without hysteresis compensation – yellow and with compensation – blue (right)

6 CONCLUSION

This paper focuses on the description of the PL140 piezoelectric actuator using both an accurate physical model and a simplified data-driven model. The physical model is built on a physical analysis and the manufacturer’s datasheets and it is intended to serve as a substitution for the original piezoelectric actuator to provide experimental data. The use of this allows for the performance of various experiments without the need for costly measuring devices and without the risk of damaging the original actuator. The developed data-driven model is meant for a future model-based micro-positioning control implementation.

The chosen identification scheme, specifically the Hammerstein model, allows for independent estimation of the linear dynamic and nonlinear static components, providing flexibility in selecting both the linear model and the function

that characterizes the nonlinear static part. The choice of the uniform ARX model was motivated mainly by the simplicity of the estimation algorithm. In addition, the knowledge of the noise bound r is unnecessary, as it is estimated simultaneously with the model parameters. A function representing the nonlinear static component was effectively identified using a shallow neural network model from MATLAB toolbox.

The above mentioned models have been presented in paper [12]. The current paper builds on the previously reported results by utilizing both parts of the proposed Hammerstein model to design a feed-forward controller. The inversion of the linear ARX model is straightforward, as it consists only in swapping its input and output. The inversion of hysteresis model utilizes a numerical technique based on a k-vector range searching. In order to use this method, we first need to divide the data describing the hysteresis curve into two parts corresponding to two non-linear functions.

Future research will focus on incorporating the proposed data-driven model and developed feed-forward controller (hysteresis compensator) into an output-feedback model predictive control scheme. Feedforward-feedback control utilizes advantages of both approaches and is typically used for high-speed and high precision operations of PEAs [10]. We also plan to test the proposed algorithms on a real piezo actuator.

Acknowledgments. This work was supported by The Czech Academy of Sciences, Institute of Information Theory and Automation under the project No. 23-04676J of the Czech Science Foundation: Controllable Gripping Mechanics: Modelling, Control and Experiments.

Disclosure of Interests. The authors have no competing interests to declare that are relevant to the content of this article.

References

1. Arnas, D., Mortari, D.: Nonlinear function inversion using k-vector. *Applied mathematics and computation* **320**, 754–768 (2018)
2. Bai, E.W.: Decoupling the linear and nonlinear parts in Hammerstein model identification. *Automatica* **40**(4), 671–676 (2004)
3. Benjeddou, A., Trindade, M.A., Ohayon, R.: A unified beam finite element model for extension and shear piezoelectric actuation mechanisms. *Journal of Intelligent Material Systems and Structures* **8**(12), 1012–1025 (1997)
4. Bruno, B.P., Fahmy, A.R., Stürmer, M., Wallrabe, U., Wapler, M.C.: Properties of piezoceramic materials in high electric field actuator applications. *Smart Materials and Structures* **28**(1), 015029 (2018)
5. Dai, Y., Li, D., Wang, D.: Review on the nonlinear modeling of hysteresis in piezoelectric ceramic actuators. *Actuators* **12**(12) (2023)
6. Gao, T., Liao, Q., Si, W., Chu, Y., Dong, H., Li, Y., Liao, Y., Qin, L.: From fundamentals to future challenges for flexible piezoelectric actuators. *Cell Reports Physical Science* **5**(2), 101789 (2024)

7. Gao, X., Ren, X., Zhu, C., Zhang, C.: Identification and control for Hammerstein systems with hysteresis non-linearity. *IET Control Theory & Applications* **9**(13), 1935–1947 (2015)
8. Hughes, T.J.: *The finite element method: linear static and dynamic finite element analysis*. Courier Corporation (2003)
9. Ismail, M., Ikhouane, F., Rodellar, J.: The hysteresis Bouc-Wen model, a survey. *Archives of computational methods in engineering* **16**, 161–188 (2009)
10. Kanchan, M., Santhya, M., Bhat, R., Naik, N.: Application of modeling and control approaches of piezoelectric actuators: A review. *Technologies* **11**(6), 155 (2023)
11. Kárný, M., Böhm, J., Guy, T.V., Jirsa, L., Nagy, I., Nedoma, P., Tesař, L.: *Optimized Bayesian Dynamic Advising: Theory and Algorithms*. Springer, London (2006)
12. Kuklišová Pavelková, L., Belda, K.: Identification of piezoelectric actuator using Bayesian approach and neural networks. In: *Proc. 21st International Conference on Informatics in Control, Automation and Robotics - Volume 1: ICINCO*. pp. 591–599. INSTICC, SciTePress (2024). <https://doi.org/10.5220/0013011700003822>
13. MathWorks: Piezo bender. www.mathworks.com/help/sps/ref/piezobender.html (2021), accessed: 2025-03-10
14. Pavelková, L., Kárný, M.: Approximate Bayesian recursive estimation of linear model with uniform noise. *IFAC Proceedings Volumes* **45**(16), 1803–1807 (2012)
15. Tadmor, E.B., Kósa, G.: Electromechanical coupling correction for piezoelectric layered beams. *Journal of Microelectromechanical Systems* **12**(6), 899–906 (2003)
16. Torsten Soderstrom, P.S.: *System identification*. Prentice Hall International Series in Systems and Control Engineering, Prentice Hall (1999)
17. Uralde, J., Artetxe, E., Barambones, O., Calvo, I., Fernandez-Bustamante, P., Martin, I.: Ultraprecise controller for piezoelectric actuators based on deep learning and model predictive control. *Sensors* **23**(3) (2023). <https://doi.org/10.3390/s23031690>
18. Wilkie, J., Johnson, M., Katebi, R.: *Simple systems: second-order systems*, pp. 173–195. Macmillan Education UK, London (2002)
19. Zhang, M., Cui, X., Xiu, Q., Zhuang, J., Yang, X.: Dynamic modeling and controlling of piezoelectric actuator using a modified preisach operator based hammerstein model. *International Journal of Precision Engineering and Manufacturing* **24**(4), 537–546 (2023)
20. Zhou, X., Wu, S., Wang, X., Wang, Z., Zhu, Q., Sun, J., Huang, P., Wang, X., Huang, W., Lu, Q.: Review on piezoelectric actuators: materials, classifications, applications, and recent trends. *Frontiers of Mech. Engin.* **19**(1), 6 (2024)